

Na⁺-dependent Cl-HCO₃ Exchange in the Squid Axon

Dependence on Extracellular pH

WALTER F. BORON and ROGER C. KNAKAL

From the Department of Cellular and Molecular Physiology, Yale University School of Medicine, New Haven, Connecticut 06510-2989

ABSTRACT Intracellular pH (pH_i) in squid giant axons recovers from acid loads by means of a Na⁺-dependent Cl-HCO₃ exchanger, the actual mechanism of which might be exchange of: (i) external Na⁺ and HCO₃⁻ for internal Cl⁻ and H⁺, (ii) Na⁺ plus two HCO₃⁻ for Cl⁻, (iii) Na⁺ and CO₃⁼ for Cl⁻, or (iv) the NaCO₃⁻ ion pair for Cl⁻. Here we examine sensitivity of transport to changes of extracellular pH (pH_o) in the range 7.1–8.6. We altered pH_o in four ways, using: (i) classical “metabolic” disturbances in which we varied [HCO₃⁻]_o, [NaCO₃⁻]_o, and [CO₃⁼]_o at a fixed [CO₂]_o; (ii) classical “respiratory” disturbances in which we varied [CO₂]_o, [NaCO₃⁻]_o, and [CO₃⁼]_o at a fixed [HCO₃⁻]_o; (iii) novel mixed-type acid–base disturbances in which we varied [HCO₃⁻]_o and [CO₂]_o at a fixed [CO₃⁼]_o and [NaCO₃⁻]_o; and (iv) a second series of novel mixed-type disturbances in which we varied [CO₂]_o, [CO₃⁼]_o, and [Na⁺]_o at a fixed [HCO₃⁻]_o and [NaCO₃⁻]_o. Axons (initial pH_i ~ 7.4) were internally dialyzed with a pH 6.5 solution containing 400 mM Cl⁻ but no Na⁺. After pH_i, measured with a glass microelectrode, had fallen to ~6.6, dialysis was halted. The equivalent acid extrusion rate (*J*_H) was computed from the rate of pH_i recovery (i.e., increase) in the presence of Na⁺ and HCO₃⁻. When pH_o was varied by method (i), which produced the greatest range of [CO₃⁼]_o and [NaCO₃⁻]_o values, *J*_H increased with pH_o in a sigmoidal fashion; the relation was fitted by a pH titration curve with a pK of ~7.7 and a Hill coefficient of ~3.0. With method (ii), which produced smaller changes in [CO₃⁼]_o and [NaCO₃⁻]_o, *J*_H also increased with pH_o, though less steeply. With method (iii), which involved changes in neither [CO₃⁼]_o nor [NaCO₃⁻]_o, *J*_H was insensitive to pH_o changes. Finally, with method (iv), which involved changes in neither [HCO₃⁻]_o nor [NaCO₃⁻]_o, but reciprocal changes in [CO₃⁼]_o and [Na⁺]_o, *J*_H also was insensitive to pH_o changes. We found that decreasing pH_o from 8.6 to 7.1 caused the apparent *K*_m for external HCO₃⁻ ([Na⁺]_o = 425 mM) to increase from 1.0 to 26.7 mM, whereas *J*_{max} was relatively stable. Decreasing pH_o from 8.6 to 7.4 caused the apparent *K*_m values for external Na⁺ ([HCO₃⁻]_o = 48 mM) to increase from 8.6 to 81 mM, whereas *J*_{max} was relatively stable. These data are consistent with the ion pair model, and severely restrict kinetic parameters for other models.

Address reprint requests to Dr. Walter F. Boron, Department of Cellular and Molecular Physiology, Yale University School of Medicine, 333 Cedar Street, New Haven, CT 06510-2989.

INTRODUCTION

In squid giant axons, the transporter responsible for recovery of intracellular pH (pH_i) from acid loads is the Na^+ -dependent Cl-HCO_3 exchanger. Characterized in squid axons (Boron and De Weer, 1976; Russell and Boron, 1976) and snail neurons (Thomas, 1976, 1977), this acid extrusion mechanism was later described in a variety of other cells, both invertebrate (Moody, 1981; Boron, McCormick, and Roos, 1981) and vertebrate (Rothenberg, Glaser, Schlesinger, and Cassel, 1983; L'Allemain, Paris, and Pouyssegur, 1985; Tonnessen, Ludt, Sandvig, and Olsnes, 1987; Boyarsky, Ganz, Sterzel, and Boron, 1988; Cassel, Scharf, Rotman, Cragoe, and Katz, 1988). The transporter seems to exchange extracellular Na^+ and HCO_3^- for intracellular Cl^- and H^+ , though the precise roster of transported ions has not been established. Three other possibilities (Boron, 1985) are that intracellular Cl^- is exchanged for: (i) extracellular Na^+ and two HCO_3^- ions, (ii) extracellular Na^+ and one CO_3^{2-} ion, and (iii) the extracellular NaCO_3^- ion pair.

Kinetic studies are one approach for understanding how the transporter may respond to physiologically relevant perturbations, as well as for probing the potential ionic mechanisms of transport. Previous kinetic work has focused on how the squid axon's Na^+ -dependent Cl-HCO_3 exchanger is affected by changes in $[\text{Na}^+]_o$ and/or $[\text{HCO}_3^-]_o$ at the single pH_o of 8.0 (Boron and Russell, 1983; Boron, 1985). The results indicate that the equivalent acid extrusion rate (J_H) is approximately governed by the product $[\text{Na}^+]_o \times [\text{HCO}_3^-]_o$. These data are most easily explained by the NaCO_3^- ion pair hypothesis, but do not exclude highly restricted versions of the other models. Another squid axon study, which focused on how the transporter's $[\text{Na}^+]_o$ and $[\text{HCO}_3^-]_o$ dependencies are affected by the reversible inhibitor 4,4'-dinitrostilbene-2,2'-disulfonate (DNDS), showed that the divalent anion DNDS appears to be a competitive inhibitor with respect to both extracellular Na^+ and HCO_3^- (Boron and Knakal, 1989). These results, too, are explained most easily by the NaCO_3^- ion pair hypothesis. Although the DNDS data do not rule out other models, these results place restrictions on these other models that are even more severe than those required by the earlier work. These data provide a framework for understanding the interaction among the Na^+ -dependent Cl-HCO_3 exchanger and extracellular Na^+ and HCO_3^- , though only at the single extracellular pH (pH_o) of 8.00. In spite of the importance of the Na^+ -dependent Cl-HCO_3 exchanger, we know relatively little about how it is affected by pH_o changes that may be important both physiologically and pathophysiologically. Work on the Na^+ -dependent Cl-HCO_3 exchanger in barnacle muscle fibers has shown that J_H is inhibited by metabolic acidosis (i.e., a reduction in $[\text{HCO}_3^-]_o$ at a fixed pCO_2). However, because HCO_3^- (or a $[\text{HCO}_3^-]$ -dependent solute such as CO_3^{2-} or NaCO_3^-) is a substrate of the transporter, the effects of metabolic acidosis provide little insight into the effect of acidosis per se.

The purpose of the present work is to analyze how changes in pH_o influence the Na^+ -dependent Cl-HCO_3 exchanger. We examine the effects of the two classical acid-base disturbances: (i) metabolic (in which $[\text{HCO}_3^-]_o$, $[\text{CO}_3^{2-}]_o$ and $[\text{NaCO}_3^-]_o$ vary, but $[\text{CO}_2]_o$ is fixed), and (ii) respiratory (in which $[\text{CO}_2]_o$, $[\text{CO}_3^{2-}]_o$, and $[\text{NaCO}_3^-]_o$ vary, but $[\text{HCO}_3^-]_o$ is fixed). However, a study of how J_H is affected by only these two disturbances, both of which involve sizable changes in $[\text{CO}_3^{2-}]_o$ and $[\text{NaCO}_3^-]_o$,

provides little insight into a mechanism that may involve CO₃²⁻ or NaCO₃⁻. Even if HCO₃⁻ were the true substrate of the transporter, a complete characterization of the transporter would require a response to the "mixed-type" acid-base disturbances that arise spontaneously or during compensation of classical metabolic and respiratory disturbances. Therefore, in this study we introduce two novel acid-base disturbances and examine how they affect Na⁺-dependent Cl-HCO₃ exchange: (iii) mixed-type 1 (in which [CO₂]_o and [HCO₃⁻]_o vary, but [CO₃²⁻]_o and [NaCO₃⁻]_o are fixed), and (iv) mixed-type 2 (in which [CO₂]_o, [CO₃²⁻]_o and [Na⁺]_o vary, but [HCO₃⁻]_o and [NaCO₃⁻]_o are fixed).

Our approach was to internally dialyze a squid axon to a low pH_i and use a pH-sensitive microelectrode to monitor the rate of pH_i recovery, from which we computed J_H . We examined how J_H is affected by pH_o changes in the range 7.1–8.6, altering pH_o according to the four approaches outlined above. In addition, we examined how changes in pH_o affect the dependence of J_H on [Na⁺]_o, [HCO₃⁻]_o, [CO₃²⁻]_o, and [NaCO₃⁻]_o. We found that reducing pH_o by a classical metabolic acidosis (method *i*) caused a steep decline in J_H , whereas reducing pH_o by a classical respiratory acidosis (method *ii*) caused a less steep decline in J_H . However, J_H was unaffected by reducing pH_o at a fixed [CO₃²⁻]_o and [NaCO₃⁻]_o (method *iii*), or by reducing pH_o at a fixed [HCO₃⁻]_o and [NaCO₃⁻]_o (method *iv*). We found that pH_o changes do not significantly affect the apparent maximal J_H . However, external acidosis causes steep increases in apparent values for $K_m(\text{Na}^+)$ and $K_m(\text{HCO}_3^-)$, without substantially affecting either $K_m(\text{CO}_3^{2-})$ or $K_m(\text{NaCO}_3^-)$. The most straightforward explanation for the data is the NaCO₃⁻ ion pair model. However, with appropriate ad hoc assumptions, and with extreme values for certain kinetic parameters, the models involving HCO₃⁻ and CO₃²⁻ also fit the data. Models aside, a useful guideline is that, regardless of pH_o, the transport rate is approximately governed by the product [Na⁺]_o × [CO₃²⁻]_o.

Portions of this work have been published in abstract form (Boron and Knakal, 1986).

METHODS

General

The experiments were conducted at the Marine Biological Laboratory, Woods Hole, MA. Live squid (*Loligo pealei*) were decapitated, and the first stellar nerve of each side was removed and placed in cold (~4°C) natural seawater. From this nerve we microdissected a 3–4-cm length of giant axon, 400–700 μm in diameter. This was cannulated horizontally in a chamber designed for internal dialysis (Brinley and Mullins, 1967); our use of the method is detailed in earlier papers (Boron and Russell, 1983; Boron, 1985). A length of cellulose acetate dialysis tubing (Fisher Research Laboratories, Dedham, MA), with an outer diameter of 140 μm, was inserted through one cannula and threaded down the axon and out the opposite cannula. This tubing was arranged so that an 18-mm length of tubing, previously permeabilized by hydrolyzing 18–24 h in 0.1 N NaOH, was centered in the axon. The dialysis capillary was perfused with dialysis fluid (DF) at a rate of ~5 μl/min. Also inserted into the axon through opposite cannulas were a voltage-sensitive and a pH-sensitive microelectrode, arranged so that their tips were centered in the axon within ~500 μm of each other. The open-tipped voltage electrode was filled with 3 M KCl. The pH-sensitive microelectrodes were of the design of Hinke (Hinke,

1967), and constructed of pH-sensitive glass (Clark Electromedical Instruments, Pangbourne, UK) and lead glass (0120; Corning Glass Works, Corning, NY). Details on the construction of the microelectrodes, the use of high-impedance electrometers and other devices to handle the electrode signals, the acquisition of data by computer, and the computer control of the experiments have been provided previously (Boron and Russell, 1983; Boron, 1985). The axon was superfused continuously with artificial seawater (ASW). The temperature was maintained at 22°C by using a circulating bath to pump water through the jacketed chamber.

Solutions

Artificial seawaters. The standard extracellular fluid was an ASW buffered to pH 8.00 and having the following composition (mM): 425.2 Na⁺, 12 K⁺, 3 Ca²⁺, 57.5 Mg²⁺, 531 Cl⁻, nominally 12 HCO₃⁻, 0.1 EDTA⁻, 15 of the anionic form of [2-hydroxyethyl]-1-piperazine-propane sulfonic acid (EPPS), and 15 of the neutral form of EPPS (pK ~ 8.0). When HCO₃⁻ is added to a solution that is initially CO₂/HCO₃⁻ free, some of the added HCO₃⁻ undergoes the reaction HCO₃⁻ + H⁺ → H₂CO₃ → CO₂ + H₂O, and some undergoes the reaction HCO₃⁻ → H⁺ + CO₃²⁻; the CO₃²⁻ can go on to form ion pairs with Ca²⁺, Mg²⁺, and Na⁺. Thus, the actual [HCO₃⁻]_o is less than the nominal [HCO₃⁻]_o. We made our standard ASW as previously described (Boron and Knakal, 1989), titrating a CO₂/HCO₃⁻-free EPPS-buffered stock solution to pH 8.00, adding NaHCO₃ (which causes a paradoxical pH decrease), and then returning pH_o to 8.00 by gassing with 0.5% CO₂/balance O₂ (thereby evolving CO₂). As described in a previous analysis (Boron and Knakal, 1989), when pH_o is 8.00, [EPPS] is 30 mM, and the nominal [HCO₃⁻]_o is 12 mM, the actual [HCO₃⁻]_o is computed to be ~10% less (i.e., ~10.8 mM). The predicted magnitude of this discrepancy increases at higher [HCO₃⁻]_o values, and increases substantially at higher pH values (Boron and Knakal, 1989). Therefore, in designing ASWs for this study, we increased the added HCO₃⁻ as necessary to keep the computed [HCO₃⁻]_o within ~10% of the nominal [HCO₃⁻]_o. The calculation of actual [HCO₃⁻]_o was done by computer, using the approach outlined previously (Boron and Knakal, 1989). This addition of extra HCO₃⁻ was necessary only for pH_o values of 8 or greater. Table I summarizes values for nominal (i.e., desired) [HCO₃⁻]_o, added [HCO₃⁻]_o, and computed [HCO₃⁻]_o for each of the 54 combinations of pH, [HCO₃⁻]_o, and [Na⁺]_o used in this study. The table also identifies which of the 13 series of experiments each solution was used in, the mean observed flux (i.e., J_{H}) ± SEM, and the number of observations from which this mean was computed. In computations of kinetic parameters, we always used computed [HCO₃⁻]_o values rather than nominal or added values.

For an extracellular buffer we chose 30 mM EPPS (pK ~ 8.0), and we established pH_o values between 7.1 and 8.6 by titrating 30 mM EPPS free acid with different amounts of MgO at 22°C. We chose to use a single buffer (rather than different buffers for different pH_o values) in order to avoid the criticism that observed changes might be buffer- rather than pH_o-dependent. On the other hand, we recognize that pH_o changes are necessarily accompanied by changes in the ratio [EPPS·H⁺]_o/[EPPS]_o. We chose EPPS as the buffer because it was used in previous studies, and because its pK is approximately in the middle of the desired pH_o range. We compensated for changes in osmolality by varying the amount of MgCl₂ added to the solutions. The osmolality of the final ASWs was adjusted as necessary to ~975 mosm/kg by the addition of H₂O or MgCl₂. The ASW was delivered to the chamber through CO₂-impermeable Saran tubing (Clarkson Equipment and Controls, Detroit, MI). When [HCO₃⁻]_o was varied, HCO₃⁻ was exchanged mole-for-mole with Cl⁻. When [Na⁺]_o was lowered, Na⁺ was replaced mole-for-mole with K⁺. Previous work (Boron and Russell, 1983) showed that the depolarization associated with increased [K⁺]_o does not affect the rate of the Na⁺-dependent Cl-HCO₃ exchanger.

Dialysis fluids. The internal dialysis fluid (DF) had the following composition (mM): 0 Na⁺, 413.3 K⁺, 7 Mg²⁺, 8 Tris⁺, 400 Cl⁻, 14 glutamate, 4 ATP⁻, 1 EGTA⁻, 13.3 of the anionic form of 2-[N-morpholino]-ethanesulfonic acid (MES), 6.7 of the neutral form of MES, 215 glycine, and 0.5 phenol red. KOH or HCl was used to titrate the pH to 6.5 at 22°C. The

TABLE I
Composition of HCO₃⁻-containing Seawaters

Solu- tion No.	Used in series No.	pH	Nominal [Na ⁺]	Nominal [CO ₂]	Nominal [HCO ₃]	Added [HCO ₃]	Computed [HCO ₃]	Computed [CO ₃]	Computed [NaCO ₃]	Flux	n
			mM	%	mM	mM	mM	μM	μM	<i>pmol</i> <i>cm⁻² s⁻¹</i>	
1	1,10	8.6	425	0.5	48	57.8	48.0	1,911	4,779	21.6 ± 2.3	7
2	2,10	8.6	425	0.125	12	16.3	12.0	478	1,194	22.4 ± 1.2	7
3	10	8.6	425	0.0625	6	8.6	6.0	238	595	21.6 ± 2.3	7
4	3,10	8.6	425	0.0313	3	4.5	3.0	119	298	17.3 ± 0.8	18
5	10	8.6	425	0.0156	1.5	2.3	1.5	59	148	13.7 ± 1.4	9
6	10	8.6	425	0.00781	0.75	1.15	0.73	29.0	72.5	8.8 ± 0.5	15
7	10	8.6	425	0.00391	0.375	0.58	0.364	14.5	36.2	6.4 ± 0.6	15
8	10	8.6	425	0.00195	0.1875	0.30	0.1873	7.5	18.6	4.1 ± 0.4	13
9	13	8.6	26.5	0.5	48	55.4	48.1	1,914	298	15.0 ± 2.3	4
10	4,13	8.6	13.25	0.5	48	55.4	48.2	1,917	149	16.0 ± 2.3	6
11	13	8.6	6.625	0.5	48	55.4	48.2	1,919	74.8	9.0 ± 1.6	10
12	13	8.6	3.313	0.5	48	55.4	48.3	1,920	37.4	4.9 ± 0.6	6
13	13	8.6	1.656	0.5	48	55.4	48.3	1,921	18.7	4.0 ± 0.5	5
14	1,9	8.3	425	0.5	24	24.0	20.0	400	1,000	18.6 ± 0.5	9
15	2,9	8.3	425	0.25	12	14.6	12.0	239	598	19.3 ± 0.7	13
16	3,9	8.3	425	0.125	6	7.4	6.0	119	298	19.0 ± 0.6	18
17	9	8.3	425	0.0625	3	3.7	3.0	59.0	148	14.7 ± 0.9	9
18	9	8.3	425	0.0313	1.5	1.85	1.5	29.3	73.4	9.6 ± 0.4	12
19	9	8.3	425	0.0156	0.75	0.93	0.74	14.7	36.8	6.5 ± 0.5	11
20	9	8.3	425	0.00781	0.375	0.47	0.372	7.4	18.6	4.9 ± 0.3	10
21	4	8.3	26.5	1.0	48	53.2	48.0	958	149	15.1 ± 2.1	9
22	11	8.0	106	2.0	48	48.0	44.8	447	279	17.5 ± 0.3	364
23	1,2,3,8	8.0	425	0.5	12	12.0	10.8	107	269	15.4 ± 0.5	7
24	8	8.0	425	0.25	6	6	5.4	53.6	134	11.3 ± 1.3	6
25	8	8.0	425	0.125	3	3	2.7	26.7	66.8	7.1 ± 0.2	6
26	8	8.0	425	0.0625	1.5	1.5	1.34	13.4	33.4	5.3 ± 0.7	8
27	8	8.0	425	0.0313	0.75	0.75	0.67	6.7	16.7	-0.4 ± 0.5	4
28	8	8.0	425	0.0156	0	0	0	0	0	17.7 ± 0.5	6
29	4,12	8.0	53	2.0	48	48.0	45.0	449	140	15.9 ± 1.6	10
30	12	8.0	26.5	2.0	48	48.0	45.1	450	70.0	11.2 ± 1.1	7
31	12	8.0	13.25	2.0	48	48.0	45.1	451	35.1	8.3 ± 0.4	7
32	12	8.0	6.625	2.0	48	48.0	45.2	451	17.6	5.6 ± 1.2	7
33	12	8.0	0	2.0	48	48.0	45.2	451	0	0.5 ± 1.1	4
34	7	7.7	425	4.0	48	48.0	45.4	227	568	19.0 ± 2.0	7
35	3,7	7.7	425	2.0	24	24.0	22.7	113	284	16.7 ± 0.7	19
36	2,7	7.7	425	1.0	12	12.0	11.3	56.7	142	13.1 ± 0.9	11
37	1,7	7.7	425	0.5	6	6.0	5.7	28.4	70.9	9.4 ± 0.8	12
38	7	7.7	425	0.25	3	3.0	2.8	14.2	35.5	7.1 ± 0.7	14
39	7	7.7	425	0.125	1.5	1.5	1.4	7.1	17.7	4.5 ± 0.7	7
40	4	7.7	106	4.0	48	48.0	46.1	231	144	15.7 ± 1.8	8
41	3,6,11	7.4	425	8.0	48	48.0	46.3	116	291	18.2 ± 1.3	14
42	6	7.4	425	4.0	24	24.0	23.2	58.3	146	13.1 ± 0.8	7
43	2,6	7.4	425	2.0	12	12.0	11.6	29.2	73.0	10.6 ± 1.1	9
44	6	7.4	425	1.0	6	6.0	5.8	14.6	36.5	8.8 ± 0.8	7
45	1,6	7.4	425	0.5	3	3.0	2.9	7.3	18.3	3.6 ± 0.7	6
46	4,11	7.4	212	8.0	48	48.0	46.7	117	146	15.5 ± 1.2	7
47	11	7.4	106	8.0	48	48.0	46.8	117	73.2	11.2 ± 0.8	6
48	11	7.4	53	8.0	48	48.0	46.9	118	36.7	8.7 ± 1.4	8
49	11	7.4	26.5	8.0	48	48.0	46.9	118	18.4	6.0 ± 0.6	6
50	11	7.4	0	8.0	48	48.0	47.0	118	0	4.0	1
51	3,5	7.1	425	32.0	96	96.0	92.9	117	292	19.7 ± 1.7	13
52	4,5	7.1	425	16.0	48	48.0	46.8	58.8	147	19.2 ± 1.7	9
53	2,5	7.1	425	4.0	12	12.0	11.8	14.8	37.0	6.8 ± 1.1	10
54	1,5	7.1	425	0.5	1.5	1.5	1.5	1.9	4.6	1.3 ± 1.5	6

osmolality was adjusted to ~ 975 mosmol/kg by addition of H_2O or glycine. On the day of the experiment, ATP was added to the DF from a 400-mM Tris/ATP stock (pH 7.0) stored at -5°C .

Calculation of Acid Extrusion Rates

As described previously (Boron and Knakal, 1989), pH_i data were acquired by computer, and rates of pH_i recovery from acid loads (dpH_i/dt) were determined from a linear curve fit to the data. Acid extrusion rate (J_H) is defined as the net efflux of H^+ (or other acid) plus the net influx of HCO_3^- (or other base), and computed as the product of dpH_i/dt , total intracellular buffering power, and volume-to-surface ratio. In each experiment, we computed fluxes from data obtained under our standard conditions,¹ as well as with up to three additional ASWs. All fluxes were corrected for initial and final drifts in the pH_i baseline, as previously described (Boron, 1985). Each corrected flux was normalized by dividing it by the flux computed for that experiment under standard conditions. Finally, these ratios of fluxes then converted to normalized absolute fluxes by multiplying by $17.5 \text{ pmol cm}^{-2} \text{ s}^{-1}$, the average acid extrusion rate observed under standard conditions in 364 axons in this and previous studies (see below). Fluxes were computed from rates of pH_i recovery obtained between pH_i values of ~ 6.6 and ~ 6.9 . We randomized the order in which solutions were presented to axons, as described previously (Boron, 1985).

Curve Fitting

In plots of the J_H vs. pH_o data, the choice of which function to use in a curve fit is somewhat arbitrary. In the case of the metabolic acid–base disturbances (series 1, Fig. 2A), the plot of J_H vs. pH_o resembled a pH titration curve with an unusually steep slope. Therefore, we chose to fit the data with a variant of a pH titration function that included a Hill coefficient. Because our data were normalized, we forced the fitted curve through a point described by our standard conditions. The unforced function has the form:

$$J = a + \frac{b}{1 + 10^{h(\text{pK} - \text{pH})}} \quad (1)$$

where h is the Hill coefficient. If the function is constrained to the normalization value J_N when the pH is the normalization pH (pH_N), then the function becomes:

$$J = J_N - \frac{b}{1 + 10^{h(\text{pK} - \text{pH}_N)}} + \frac{b}{1 + 10^{h(\text{pK} - \text{pH})}} \quad (2)$$

In our experiments, the pH_N was 8.00 and J_N was $17.5 \text{ pmol cm}^{-2} \text{ s}^{-1}$, the average acid extrusion rate observed under standard conditions in 364 axons. As a control, we not only fitted normalized series 1 data with Eq. 2, we also fitted unnormalized series 1 data with Eq. 1. The results were very similar, except that the standard deviations were larger with the unnormalized data.

Because the plot of J_H vs. pH_o for the respiratory acid–base disturbances (series 2, Fig. 2B) did not clearly resemble a pH titration curve, and because there was no theoretical reason to expect the data to be fitted by any other function, we chose to fit these data with a variant of a second-order polynomial that forced the data through a point that described our standard conditions. Because the plots of J_H vs. pH_o for the mixed-type acid–base disturbances (series 3

¹ Standard conditions: $[\text{Na}^+]_o = 425 \text{ mM}$, $\text{pH}_o = 8.00$, nominal $[\text{HCO}_3^-]_o = 12 \text{ mM}$ (computed $[\text{HCO}_3^-]_o = 10.8 \text{ mM}$), nominal $[\text{CO}_2]_o = 0.5\%$, $[\text{Cl}^-]_i = 400 \text{ mM}$, nominal $[\text{ATP}]_i = 4 \text{ mM}$.

and 4, Fig. 2 C) appeared linear, we chose to fit these data with a variant of a linear fit that forced the data through a point that described our standard conditions.

Values for apparent K_m and J_{max} were derived from iterative least-squares curve fits, and are presented \pm the standard deviation. In all fits of J_H vs. $[\text{HCO}_3^-]_o$, $[\text{CO}_3^{2-}]_o$, or $[\text{NaCO}_3^-]_o$, the value of the independent variable was taken as the "computed" value listed in Table I. All fits of J_H vs. $[\text{Na}^+]_o$ were nonlinear least-squares fits of the Michaelis-Menten equation. In the fit of J_H vs. $[\text{HCO}_3^-]_o$ at a pH_o of 8.0, the Michaelis-Menten curve was forced through the normalization point described by $[\text{HCO}_3^-]_o = 10.8$ mM (the computed $[\text{HCO}_3^-]_o$ under standard conditions) and $J_N = 17.5$ pmol $\text{cm}^{-2} \text{s}^{-1}$, as described previously for a "type 2 fit" (Boron, 1985). For the remainder of the fits of J_H vs. $[\text{HCO}_3^-]_o$, we used the unnormalized Michaelis-Menten equation. In the fit of J_H vs. $[\text{NaCO}_3^-]_o$ at the single pH_o of 8.0, as well as in the two fits of J_H vs. $[\text{NaCO}_3^-]_o$ that encompassed data obtained at all pH_o values, the curves were forced through the normalization point described by $[\text{NaCO}_3^-]_o = 269$ μM (the computed $[\text{NaCO}_3^-]_o$ under standard conditions) and $J_N = 17.5$ pmol $\text{cm}^{-2} \text{s}^{-1}$, as described previously for a type 2 fit (Boron, 1985).

Previously Reported Data

The present work is part of a larger study of the kinetics of the Na^+ -dependent Cl-HCO_3 exchanger in the squid giant axon (see Boron, 1985; Boron and Knakal, 1989). The average acid extrusion rate observed under standard conditions (J_N in Eq. 2) was taken as the mean value obtained in 63 (Boron, 1985) and 106 (Boron and Knakal, 1989) axons reported previously, as well as 195 axons described for the first time in the present study. Thus, the average J_H in 364 axons was 17.5 ± 0.3 pmol $\text{cm}^{-2} \text{s}^{-1}$. Because J_H data in each experiment were normalized so that J_H had a value of 17.5 pmol $\text{cm}^{-2} \text{s}^{-1}$ under standard conditions, the present data should be directly comparable to data obtained previously. The J_H vs. $[\text{HCO}_3^-]_o$ data obtained at a pH_o of 8.0 and $[\text{Na}^+]_o$ of 425 mM were reported previously (Boron, 1985), as were some of the J_H vs. $[\text{Na}^+]_o$ data obtained at a pH_o of 8.0 and a $[\text{HCO}_3^-]_o$ of 12 mM. Similarly, the J_H vs. $[\text{Na}^+]_o$ data obtained at a pH_o of 8.0 and a $[\text{HCO}_3^-]_o$ of 48 mM were reported previously (Boron and Knakal, 1989).

Statistics

Apparent values of K_m and J_{max} (see above) are expressed \pm the standard deviation. Other data (e.g., mean J_H values) are expressed \pm SEM.

RESULTS

Dependence of Acid Extrusion Rate on pH_o

We studied the effects on J_H of altering pH_o in four different ways. The first two were the classical "metabolic" and "respiratory" acid-base disturbances. The third was a novel mixed-type acid-base disturbance designed to vary pH_o at fixed values of $[\text{CO}_3^{2-}]_o$ and $[\text{NaCO}_3^-]_o$. The fourth was also a novel mixed-type acid-base disturbance in which pH_o varied at fixed values of $[\text{HCO}_3^-]_o$ and $[\text{NaCO}_3^-]_o$. The parameters varied and fixed in each of these four series of experiments are summarized in Table II.

Varying $[\text{HCO}_3^-]_o$ at constant $[\text{CO}_2]_o$: "metabolic" acid-base disturbances (series 1).

Fig. 1 illustrates an experiment in which we investigated the effects of varying pH_o on the recovery of pH_i from an acid load. The axon was initially bathed in a pH 8.00 $\text{CO}_2/\text{HCO}_3^-$ -free ASW. Internal dialysis with a fluid having a pH of 6.5 caused pH_i to

fall from ~ 7.4 to ~ 6.55 over a period of ~ 40 min (segment *ab*). After dialysis was halted, pH_i slowly increased and then leveled off (*bc*). The slope of the pH_i record (dpH_i/dt) just before point *c* is an index of the acid extrusion rate (J_H) during this initial background period.² The subsequent introduction of an ASW buffered to pH 8.3 with 24 mM HCO_3^- and 0.5% CO_2 caused a small and transient pH_i decline (*cd*), due to the influx of CO_2 , followed by a rapid alkalization (*de*), due to Na^+ -dependent Cl-HCO_3 exchange.³ Lowering pH_o from 8.3 to 7.7, achieved by reducing $[\text{HCO}_3^-]$ to 6 mM at a fixed $[\text{CO}_2]$ of 0.5%, lowered dpH_i/dt (*ef*). On the other hand, raising pH_o to 8.00 by increasing $[\text{HCO}_3^-]_o$ to 12 mM at a fixed $[\text{CO}_2]$ of 0.5% (*fg*) caused dpH_i/dt to increase, although not to a value as high as at pH_o 8.3. When pH_o was reduced to 7.4 by lowering $[\text{HCO}_3^-]_o$ to 3 mM at a fixed $[\text{CO}_2]$ of 0.5% (*gh*), dpH_i/dt decreased to a very low value. Finally, returning the axon to the control, $\text{CO}_2/\text{HCO}_3^-$ -free ASW caused a rapid alkalization (*hi*), reflecting the efflux of CO_2 , followed by a slow and steady pH_i decline (*ij*) due to a background acidifying process.

The results of 40 J_H determinations are summarized in Fig. 2*A*, which describes how the Na^+ -dependent Cl-HCO_3 exchanger was affected by metabolic acid-base disturbances. Of the four acid-base disturbances, this method of varying pH_o

TABLE II
Parameter Values in the Four Acid-Base Disturbances

Acid-base disturbance	pH_o	$[\text{CO}_2]_o$	$[\text{HCO}_3^-]_o$	$[\text{CO}_3^{2-}]$	$[\text{Na}^+]_o$	$[\text{NaCO}_3^-]_o$	J_H
		%	mM	μM	mM	μM	$\text{pmol cm}^{-2} \text{s}^{-1}$
Metabolic	7.1–8.6	Fixed: 0.5	1.5–48	1.9–1,911	Fixed: 425	4.6–4,779	1.3–21.6
Respiratory	7.1–8.6	4–0.125	Fixed: 12	14.8–478	Fixed: 425	37.0–1,194	6.8–22.4
Mixed-type 1	7.1–8.6	32–0.0313	96–3	Fixed: ~ 115	Fixed: 425	Fixed: ~ 289	15.4–19.7
Mixed-type 2	7.1–8.6	16–0.5	Fixed: 48	58.8–1,917	425–13.25	Fixed: ~ 146	15.1–19.2

produced the greatest range of $[\text{CO}_3^{2-}]_o$ values ($\sim 1,000$ -fold, from 1.9 to 1,911 μM) and $[\text{NaCO}_3^-]_o$ values (also $\sim 1,000$ -fold, from 4.6 to 4,779 μM). It also elicited the largest changes in J_H (see Table II). The curve drawn through the points is a normalized best-fit curve for a pH titration having an apparent pK_a of 7.74 and an apparent Hill coefficient of 2.98. As described in Methods, the function was forced through the point (indicated by the asterisk) describing our standard conditions ($\text{pH}_o = 8.00$, $J_H = 17.5 \text{ pmol cm}^{-2} \text{ s}^{-1}$). It can be shown that the slope of the fitted curve is maximal when $\text{pH}_o = \text{pK}$, so that the maximal fitted slope for our data is $31.5 \text{ pmol cm}^{-2} \text{ s}^{-1}$ per pH unit at a pH_o of 7.74.

² This initial background (just before point *c* in Fig. 1), as well as the final background (segment *ij* in Fig. 1), are treated as fluxes, although they could reflect intracellular events (e.g., metabolism) in whole or in part.

³ In computing J_H , we corrected for drift in the pH_i baseline by subtracting an estimate of the background J_H from the observed J_H , as described previously (Boron, 1985). In brief, we computed "initial" and "final" backgrounds as described in footnote 2, and assumed that the background flux varied linearly with time between these initial and final periods.

Varying $[CO_2]_o$ at constant $[HCO_3^-]_o$: "respiratory" acid-base disturbances (series 2). In 50 additional J_H determinations, made according to the protocol used in Fig. 1, we varied pH_o at a fixed $[HCO_3^-]_o$ of 12 mM. Compared with the metabolic disturbances, such respiratory acid-base disturbances involved smaller changes in $[CO_3^{2-}]_o$ (~32-fold, from 14.8 to 478 μ M) and $[NaCO_3^-]_o$ (also ~32-fold, from 37 to 1,194 μ M). These metabolic disturbances also elicited smaller variations in J_H (see Table II). The curve drawn through the data in Fig. 2 B is the result of a second-order polynomial curve fit that was forced through the standard point ($pH_o = 8.00$, $J_H = 17.5$ $\text{pmol cm}^{-2} \text{s}^{-1}$). The slope of the fitted function varies linearly but inversely with pH_o . The maximal slope is thus at the lowest pH_o studied, 7.1; at this pH_o , the slope is 14.8 $\text{pmol cm}^{-2} \text{s}^{-1}$ per pH unit, which is slightly less than half as great as the maximal slope of the fitted curve describing the metabolic acid-base disturbances (Fig. 2 A).

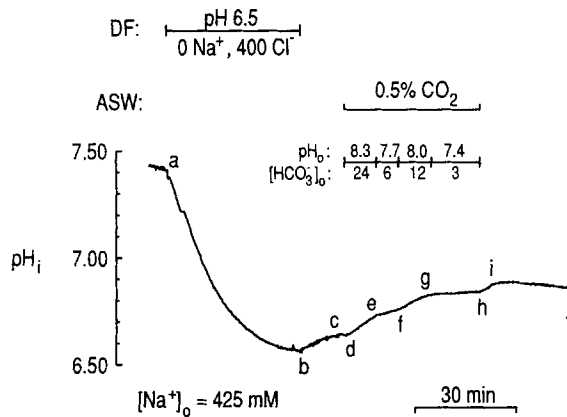


FIGURE 1. Recovery of pH_i from an acid load, and the effect of varying $[HCO_3^-]_o$ at a fixed $[CO_2]_o$ of 0.5%. The axon (a050485d), which had an initial pH_i of 7.42, was acid loaded by dialyzing between points *a* and *b* with a pH 6.5 solution having a $[Na^+]$ of 0 mM and a $[Cl^-]$ of 400 mM. After pH_i had stabilized in the absence of CO_2/HCO_3^- at *c*, we monitored the pH_i recovery in the presence of CO_2/HCO_3^- at pH_o values of 8.3 ($[HCO_3^-]_o = 24$ mM),

7.7 ($[HCO_3^-]_o = 6$ mM), 8.0 ($[HCO_3^-]_o = 12$ mM), and 7.4 ($[HCO_3^-]_o = 3$ mM). Finally, at *h* we returned the axon to a CO_2/HCO_3^- -free seawater. The axon diameter was 600 μ m.

Varying $[HCO_3^-]_o$ and $[CO_2]_o$ at constant $[CO_3^{2-}]_o$ and $[NaCO_3^-]_o$: first mixed-type acid-base disturbance (series 3). In the first two series of experiments, variations in pH_o were accompanied by changes in both $[CO_3^{2-}]_o$ and $[NaCO_3^-]_o$. In the third series, we varied pH_o by altering $[HCO_3^-]_o$ and $[CO_2]_o$ in such a way that $[CO_3^{2-}]_o$ was held fixed at ~115 μ M, $[NaCO_3^-]_o$ at ~289 μ M, and $[Na^+]_o$ at ~425 mM. As summarized in Fig. 2 C for 82 determinations of J_H , this acid-base disturbance only slightly affected J_H , which tended to fall as pH_o rose. The regression line forced through the standard point ($pH_o = 8.00$, $J_H = 17.5$ $\text{pmol cm}^{-2} \text{s}^{-1}$) has a slope of -0.8 ± 0.8 $\text{pmol cm}^{-2} \text{s}^{-1}$ per pH unit. This slope is of the opposite sign and only ~2.5% of the magnitude of the maximal slope in series 1.

Varying $[CO_2]_o$ and $[Na^+]_o$ at constant $[HCO_3^-]_o$ and $[NaCO_3^-]_o$: second mixed-type acid-base disturbance (series 4). Although J_H was not significantly affected by pH_o changes in the series 3 data, the experiments did not distinguish among $[CO_3^{2-}]_o$, $[NaCO_3^-]_o$, and $[Na^+]_o$, which were all fixed. We therefore examined the effects of a second mixed-type disturbance, one in which we varied pH_o by altering $[Na^+]_o$ (~32-fold, from 425 to 13.25 mM), $[CO_2]_o$ (32-fold, from 16 to 0.5%), and $[CO_3^{2-}]_o$

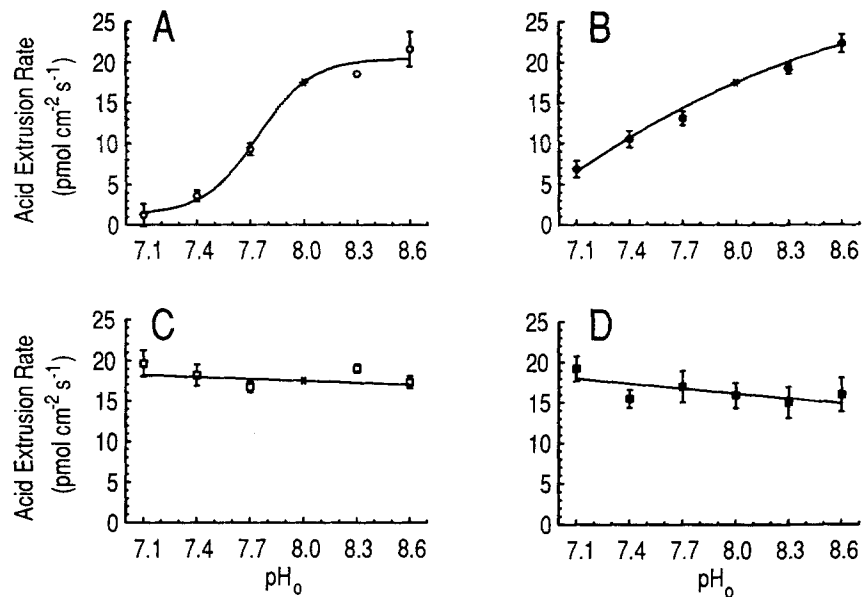


FIGURE 2. Dependence of acid extrusion rate on extracellular pH for four types of acid-base disturbances. (A) Metabolic acid-base disturbances (series 1). The J_H data are indicated by open circles. The error bars indicate the SEM; error bars are omitted for SEMs that were less than half the vertical size of the symbol. The curve drawn through the points is the result of a nonlinear least-squares curve fit of the data by Eq. 2 (see Methods) that forces the curve through a point (*asterisk*) describing our standard conditions. Best-fit values were $b = 18.6 \pm 1.76$, $pK = 7.74 \pm 0.04$, and $h = 2.98 \pm 0.53$ ($n = 40$). (B) Respiratory acid-base disturbances (series 2). The J_H data are indicated by filled circles. The curve drawn through the points is the result of a least-squares curve fit of the data by a second-order polynomial (see Methods) that forces the curve through a point (*asterisk*) describing our standard conditions. Best-fit values for the polynomial $J_H = a_0 + a_1 \times pH_o + a_2 \times (pH_o)^2$ were $a_0 = -244.9$, $a_1 = 56.04$, and $a_2 = -2.906$ ($n = 50$). (C) Mixed-type acid-base disturbance 1 (series 3). The J_H data are indicated by open squares. The curve drawn through the points is the result of a least-squares curve fit of the data by a line that is forced through a point (*asterisk*) describing our standard conditions. Best-fit values for the line $J_H = a_0 + a_1 \times pH_o$ were $a_0 = 23.97$ and $a_1 = -0.8085$ ($n = 82$). (D) Mixed-type acid-base disturbance 2 (series 4). The J_H data are indicated by filled squares. The curve drawn through the points is the result of a least-squares curve fit of the data by the line $J_H = a_0 + a_1 \times pH_o$, where $a_0 = 32.5$ and $a_1 = -2.046$ ($n = 50$).

(~ 33 -fold, from 58.8 to 1,917 μM) in such a way that $[HCO_3^-]_o$ was held fixed at 48 mM and $[NaCO_3^-]_o$ at ~ 146 μM . The results of 50 such J_H determinations, summarized in Fig. 2 D, again show that the Na^+ -dependent $Cl-HCO_3$ exchanger was not substantially affected by changes in pH_o , though J_H showed a small tendency to decline with increasing values of pH_o . The regression line, not forced through a standard point, has a slope of -2.0 ± 1.4 $pmol\ cm^{-2}\ s^{-1}$ per pH unit. This value has the opposite sign and only $\sim 6\%$ of the magnitude of the maximum slope in series 1.

Effect of pH_o Changes on the Transporter's Apparent [NaCO₃⁻]_o, [HCO₃⁻]_o, [CO₃⁼]_o, and [Na⁺]_o Dependencies

[NaCO₃⁻]_o. The above data indicate that varying pH_o in the range 7.1–8.6 has no substantial effect on J_H , provided that the product of [CO₃⁼]_o and [Na⁺]_o (and thus [NaCO₃⁻]_o) is held constant. If the NaCO₃⁻ ion pair were the extracellular substrate of the Na⁺-dependent Cl-HCO₃ exchanger, and if the exchanger were unaffected by changes in pH_o per se, then J_H would depend uniquely on [NaCO₃⁻]_o, regardless of pH_o. In Fig. 3 we have replotted the J_H data of Fig. 2, *A–D* as a function of [NaCO₃⁻]_o, retaining the same symbols as in Fig. 2. It is apparent that the data for all four series of experiments (i.e., the four methods for varying pH_o) are consistent with a single dependence of J_H on [NaCO₃⁻]_o. The curve drawn through the data in Fig. 3

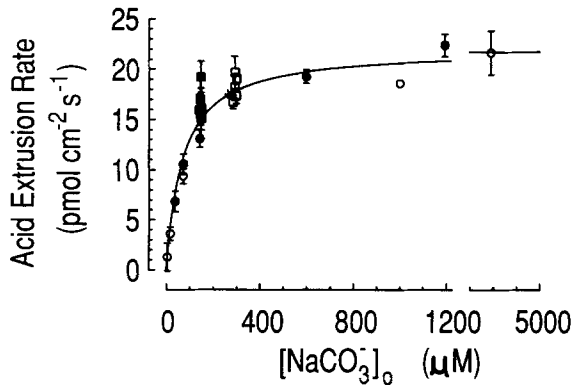


FIGURE 3. Dependence of acid extrusion rate on [NaCO₃⁻]_o. The J_H data depicted in Fig. 2, *A–D* are replotted as a function of [NaCO₃⁻]_o. As in the previous figure, the open circles represent data from series 1 (Fig. 2*A*); the filled circles, series 2 (Fig. 2*B*); the open squares, series 3 (Fig. 2*C*); and the filled squares, series 4 (Fig. 2*D*). The curve drawn through the points is the result of a nonlinear least-squares fit that forced the curve through our standard

conditions ([NaCO₃⁻]_o = 269 μM, J_H = 17.5 pmol cm⁻² s⁻¹; point indicated by an asterisk near the cluster of open squares). The best-fit K_m was 69 ± 9 μM, from which was computed a J_{max} of 22.0 pmol cm⁻² s⁻¹ (n = 222 J_H determinations). We obtained similar kinetic constants when we fitted all of the data presented in this study (including the additional data summarized in Figs. 4 and 5): the best-fit K_m was 79 ± 5 μM, from which was computed a J_{max} of 22.6 pmol cm⁻² s⁻¹ (n = 471).

is the result of using a nonlinear least-squares curve fitting procedure to fit the Michaelis-Menten equation simultaneously to all the data of Fig. 2, *A–D*. The apparent K_m for NaCO₃⁻ is 69 μM and the J_{max} is 22.0 pmol cm⁻² s⁻¹.

We have also examined the apparent dependence of J_H on [NaCO₃⁻]_o separately for pH_o values between 7.4 and 8.6. For this analysis, we included all of the data of Fig. 2, as well as additional data (presented below) specifically gathered for a study of the effects of pH_o changes on the [HCO₃⁻]_o and [Na⁺]_o dependencies of acid extrusion. The results, summarized in Table III, show that decreasing pH_o from 8.3 to 7.4 has virtually no effect on the apparent J_{max} (NaCO₃⁻). When pH_o is decreased from 8.6 to 8.3, J_{max} (NaCO₃⁻) increases to a value that is ~10% higher than the mean J_{max} (NaCO₃⁻) (i.e., 21.5 pmol cm⁻² s⁻¹) between pH_o 7.1 and 8.3. As was the case for J_{max} (NaCO₃⁻), K_m (NaCO₃⁻) was not very sensitive to changes in pH_o. Decreasing pH_o

from 8.3 to 7.4 had no consistent effect on $K_m(\text{NaCO}_3^-)$. The $K_m(\text{NaCO}_3^-)$ at pH_o 8.6 was ~58% higher than the average $K_m(\text{NaCO}_3^-)$ (i.e., ~68 mM) in the pH_o range from 7.4 to 8.3.

If the NaCO_3^- ion pair hypothesis were correct, then our data would imply that the Na^+ -dependent Cl-HCO_3^- exchanger itself is not very pH_o sensitive in the range 7.1–8.6. This conclusion would lead to two kinetic predictions. First, when J_H is examined as a function of $[\text{HCO}_3^-]_o$ at a fixed $[\text{Na}^+]_o$, the apparent $K_m(\text{HCO}_3^-)$ value should approximately double for each 0.3 fall in pH_o , whereas the apparent $J_{\max}(\text{HCO}_3^-)$ values should be invariant of pH_o . The basis of this prediction is that $[\text{CO}_3^{2-}]_o$ (and thus $[\text{NaCO}_3^-]_o$) should fall by half for each 0.3 fall in pH . Second, when J_H is examined as a function of $[\text{Na}^+]_o$ at a fixed $[\text{HCO}_3^-]_o$, the apparent $K_m(\text{Na}^+)$ value should approximately double for each 0.3 fall in pH_o , whereas the apparent $J_{\max}(\text{Na}^+)$ values should be stable. As noted in the Discussion, predictions experimentally indistinguishable from these are made by models calling for a separate binding

TABLE III
Effect of Altering pH_o on the $[\text{NaCO}_3^-]_o$ Dependence of Acid Extrusion

pH_o	Range of $[\text{NaCO}_3^-]_o$	$K_m(\text{NaCO}_3^-)$	J_{\max}	n
	μM	μM	$\text{pmol cm}^{-2} \text{s}^{-1}$	
7.4	0–291	64 ± 12	21.5 ± 1.5	71
7.7	18–568	78 ± 14	21.5 ± 1.2	78
8.0	0–279	54 ± 6	21.1	72
8.3	37–1,000	75 ± 9	21.9 ± 0.7	91
8.6	19–4,779	107 ± 12	23.7 ± 0.9	121

$K_m(\text{NaCO}_3^-)$ is the apparent Michaelis constant, and J_{\max} is the apparent maximal acid extrusion rate. The values of $[\text{NaCO}_3^-]_o$ were computed from the nominal $[\text{Na}^+]_o$, $[\text{HCO}_3^-]_o$, pH_o , and other parameters as described in Methods. The data at pH_o 8.0 were fitted by a normalized Michaelis-Menten equation that forced the curve through the point dictated by our standard conditions (i.e., $[\text{NaCO}_3^-]_o = 269 \mu\text{M}$, $J_H = 17.5 \text{ pmol cm}^{-2} \text{ s}^{-1}$). The data at other pH_o values were fitted by the Michaelis-Menten equation. The curve-fitting procedures, the results of which are summarized in this table, were performed on a compendium of all data reported in other tables and figures in the paper. n is the number of data points fitted.

of Na^+ and HCO_3^- (or CO_3^{2-}) in an ordered or random fashion. However, these other models make these predictions only when endowed with extreme kinetic parameters (Boron and Knakal, 1989), and only when certain ad hoc assumptions are made (see Discussion). We examined these predictions in the kinetic studies described below. The kinetic analyses incorporate the data summarized in Fig. 2, A–D, as well as additional data gathered according to the protocol of Fig. 1.

$[\text{HCO}_3^-]_o$. We examined the $[\text{HCO}_3^-]_o$ dependence of acid extrusion in a total of 355 J_H determinations at pH_o values of 7.1 (series 5), 7.4 (series 6), 7.7 (series 7), 8.0 (series 8), 8.3 (series 9), and 8.6 (series 10). In these experiments, $[\text{Na}^+]_o$ was fixed at 425 mM and $[\text{HCO}_3^-]_o$ was varied at a constant pH_o by making proportional changes in $[\text{HCO}_3^-]_o$ and $[\text{CO}_2]_o$. As discussed below, this approach necessarily produces changes in $[\text{CO}_3^{2-}]_o$ that are proportional to those in $[\text{HCO}_3^-]_o$. The dependence of J_H on $[\text{HCO}_3^-]_o$ at each of these pH_o values is plotted in Fig. 4 A. The best-fit values for $K_m(\text{HCO}_3^-)$ and $J_{\max}(\text{HCO}_3^-)$ are plotted as a function of pH_o in Fig. 4 B, and are

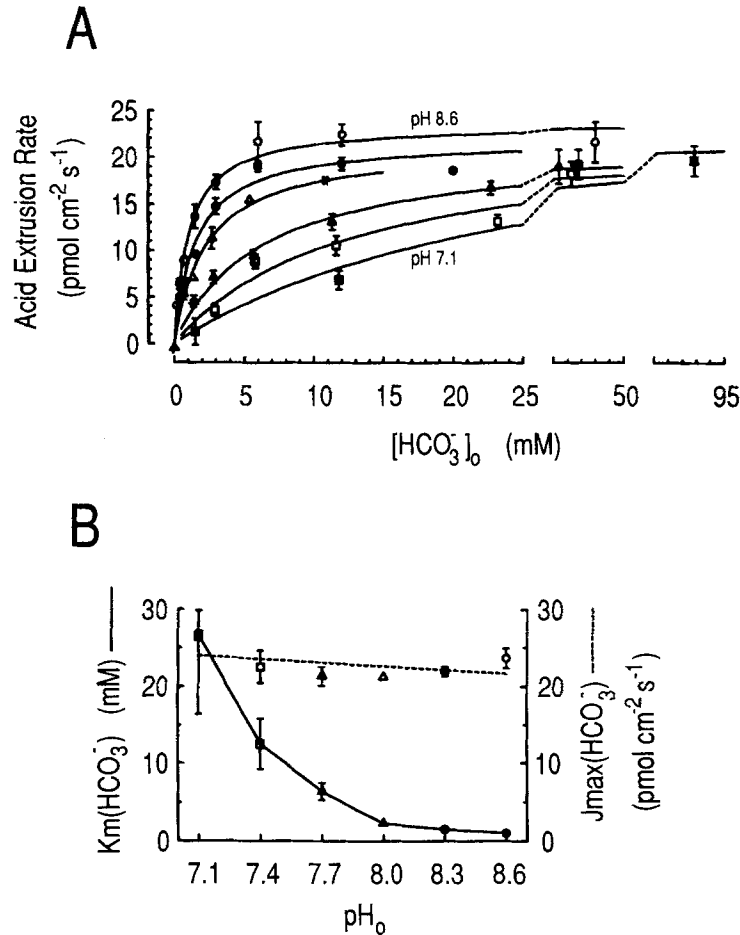


FIGURE 4. Effect of changes in pH_o on the $[\text{HCO}_3^-]_o$ dependence of the Na^+ -dependent Cl-HCO_3 exchanger. (A) Dependence of acid extrusion rate on $[\text{HCO}_3^-]_o$ at different values of pH_o . The top data set (*open circles*) was obtained at pH_o 8.6, and the bottom set (*filled squares*) at a pH_o of 7.1. The intermediated data sets were obtained at pH_o values of 8.3 (*filled circles*), 8.0 (*open triangles*), 7.7 (*filled triangles*), and 7.4 (*open squares*). The curves drawn through the points are the result of nonlinear least-squares curve fits to J_H vs. $[\text{HCO}_3^-]_o$, the results of which are summarized in Table IV. The fit at pH_o 8.0 was to a modified form of the Michaelis-Menten equation that forced the curve through the point (*asterisk*) defined by our standard conditions ($[\text{HCO}_3^-]_o = 10.8$ mM, $J_H = 17.5$ pmol cm^{-2} s^{-1}). (B) Dependence of $K_m(\text{HCO}_3^-)$ and $J_{\max}(\text{HCO}_3^-)$ on pH_o . The kinetic parameters from the curve fits are plotted as a function of pH_o . The symbols are the same as in A. The solid squares representing $K_m(\text{HCO}_3^-)$ and $J_{\max}(\text{HCO}_3^-)$ at pH_o 7.1 overlay one another; the error bar extending upward from this solid square refers to the $J_{\max}(\text{HCO}_3^-)$ value, the one extending downward, the $K_m(\text{HCO}_3^-)$ value. The $K_m(\text{HCO}_3^-)$ data are connected by solid line segments. The $J_{\max}(\text{HCO}_3^-)$ data were fitted to a straight line (*broken curve*).

TABLE IV
Effect of Altering pH_o on the $[HCO_3^-]_o$ Dependence of Acid Extrusion in the Presence of 425 mM External Na^+

pH_o	Range of $[HCO_3^-]_o$ mM	$K_m(HCO_3^-)$ mM	J_{max} $\mu mol\ cm^{-2}\ s^{-1}$	n
7.1	1.5–92.9	26.7 ± 10.3	26.5 ± 3.4	38
7.4	2.9–46.3	12.5 ± 3.3	22.5 ± 2.1	43
7.7	1.4–45.4	6.4 ± 1.1	21.3 ± 1.2	70
8.0	0–10.8	2.3 ± 0.3	21.2	31
8.3	0.4–20	1.5 ± 0.2	21.9 ± 0.6	82
8.6	0.2–48.0	1.0 ± 0.1	23.6 ± 1.3	91

$K_m(HCO_3^-)$ is the apparent Michaelis constant and J_{max} is the apparent maximal acid extrusion rate. The values of $[HCO_3^-]_o$ were computed from the nominal $[HCO_3^-]_o$, pH_o , and other parameters as described in Methods. At each pH_o , $[HCO_3^-]_o$ was varied by proportionally varying both $[HCO_3^-]_o$ and $[CO_2]_o$. The data obtained at pH_o 8.00 were reported previously (Boron, 1985), and were fitted by a normalized Michaelis-Menten equation that forced the curve through the point by our standard conditions (i.e., $[HCO_3^-]_o = 10.8$ mM, $J_H = 17.5$ $\mu mol\ cm^{-2}\ s^{-1}$). The data at other pH_o values were fitted by the Michaelis-Menten equation. n is the number of data points fitted.

summarized in Table IV. Whereas lowering pH_o from 8.6 to 7.1 had little effect on $J_{max}(HCO_3^-)$, the trend being to slightly increase $J_{max}(HCO_3^-)$, this decrease in pH_o produced a marked increase in $K_m(HCO_3^-)$. As predicted by the ion pair model, each 0.3 reduction in pH_o caused an approximate doubling of $K_m(HCO_3^-)$ between pH_o values of 8.3 and 7.1. $K_m(HCO_3^-)$ fell by only 50% between pH_o values of 8.6 and 8.3.

$[CO_3^{2-}]_o$. We have also fitted these J_H data from series 5 through series 10 as a function of $[CO_3^{2-}]_o$ rather than as a function of $[HCO_3^-]_o$. The results of these J_H vs. $[CO_3^{2-}]_o$ fits are summarized in Table V. As was the case for $J_{max}(HCO_3^-)$, $J_{max}(CO_3^{2-})$ did not vary substantially with pH_o in the range 8.6–7.1. However, unlike the $K_m(HCO_3^-)$ values, the $K_m(CO_3^{2-})$ values were relatively insensitive to changes in pH_o .

TABLE V
Effect of Altering pH_o on the $[CO_3^{2-}]_o$ Dependence of Acid Extrusion in the Presence of 425 mM External Na

pH_o	Range of $[CO_3^{2-}]_o$ μM	$K_m(CO_3^{2-})$ μM	J_{max} $\mu mol\ cm^{-2}\ s^{-1}$	n
7.1	2–117	34.1 ± 13.2	26.6 ± 3.4	38
7.4	7–116	31.5 ± 8.4	22.6 ± 2.1	43
7.7	7–227	31.9 ± 5.3	21.3 ± 1.2	70
8.0	0–54	23.2 ± 2.5	21.3	31
8.3	7–400	30.2 ± 3.1	21.9 ± 0.6	82
8.6	8–1,911	42.7 ± 5.1	23.6 ± 0.8	91

The data are the same as those summarized in Table IV, except that the curve fitting has been repeated with $[CO_3^{2-}]_o$ as the independent variable. $K_m(CO_3^{2-})$ is the apparent Michaelis constant and J_{max} is the apparent maximal acid extrusion rate. The values of $[CO_3^{2-}]_o$ were computed from the added $[HCO_3^-]_o$, pH_o , and other parameters, as described in Methods. The data obtained at pH_o 8.00 were fitted by a normalized Michaelis-Menten equation that forced the curve through the point dictated by our standard conditions (i.e., $[CO_3^{2-}]_o = 447$ μM , $J_H = 17.5$ $\mu mol\ cm^{-2}\ s^{-1}$); for the other data in that fit, $[CO_3^{2-}]_o$ ranged from 0 to 54 μM . The data at other pH_o values were fitted by Michaelis-Menten equation. n is the number of data points fitted.

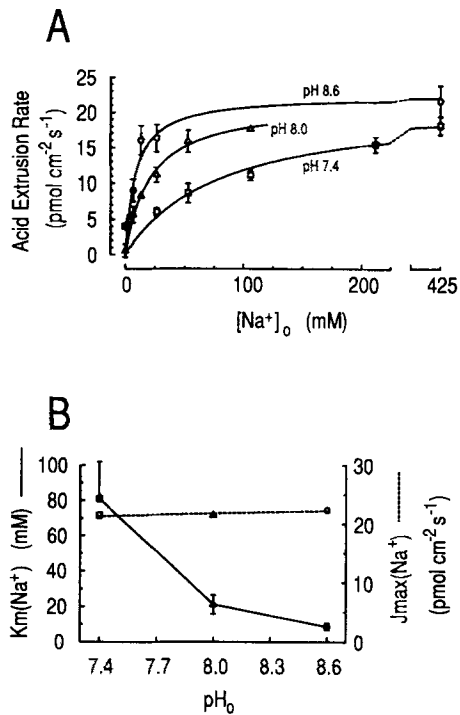


FIGURE 5. Effect of changes in pH_o on the [Na⁺]_o dependence of the Na⁺-dependent Cl-HCO₃ exchanger. (A) Dependence of acid extrusion rate on [Na⁺]_o at different values of pH_o. The top data set (*open circles*) was obtained at pH_o 8.6, the middle set (*open triangles*) at pH_o 8.0, and the bottom set (*open squares*), at pH_o 7.4. The curves drawn through the points are the result of nonlinear least-squares curve fits to J_H vs. [Na⁺]_o, the results of which are summarized in Table VI. (B) Dependence of $K_m(\text{Na}^+)$ and $J_{\max}(\text{Na}^+)$ on pH_o. The kinetic parameters from the curve fits are plotted as a function of pH_o. The symbols are the same as in A. The $K_m(\text{Na}^+)$ data are connected by solid line segments. The $J_{\max}(\text{Na}^+)$ data were fitted to a straight line (*broken curve*).

[Na⁺]_o. We examined the [Na⁺]_o dependence of acid extrusion in a total of 120 J_H determinations at pH_o values of 7.4 (series 11), 8.0 (series 12), and 8.6 (series 13). For this study, [HCO₃⁻]_o was fixed at 48 mM and the different pH_o values were established by varying [CO₂]_o. This approach necessarily involves changes in [CO₃²⁻]_o, which ranged from ~117 μM at pH_o 7.1 to ~1,917 μM at pH_o 8.6. The dependence of J_H on [Na⁺]_o at each of these pH_o values is plotted in Fig. 5 A. The best-fit values for $K_m(\text{Na}^+)$ and $J_{\max}(\text{Na}^+)$ are plotted as a function of pH_o in Fig. 5 B and summarized in Table VI. Decreasing pH_o from 8.6 to 7.4 had only a slight effect on $J_{\max}(\text{Na}^+)$, the trend being to slightly decrease $J_{\max}(\text{Na}^+)$. However, this decrease in pH_o produced a marked increase in $K_m(\text{Na}^+)$, with the 0.6 pH unit decrease from

TABLE VI
Effect of Altering pH_o on the [Na⁺]_o Dependence of Acid Extrusion in the Presence of 48 mM External HCO₃⁻

pH _o	Range of [Na ⁺] _o	$K_m(\text{Na}^+)$	J_{\max}	<i>n</i>
	<i>mM</i>	<i>mM</i>	<i>pmol cm⁻² s⁻¹</i>	
7.4	0–425	81 ± 21	21.5 ± 1.7	42
8.0	0–106	21.0 ± 5.3	21.5 ± 1.9	41
8.6	1.7–425	8.6 ± 1.9	22.4 ± 1.6	37

$K_m(\text{Na}^+)$ is the apparent Michaelis constant and J_{\max} is the apparent maximal acid extrusion rate. Some of the data (31 of 41 points) at pH_o 8.00 were reported previously (Boron and Knakal, 1989); all data at this pH_o were fitted by a normalized Michaelis-Menten equation that force the curve through the point dictated by our standard conditions (i.e., [HCO₃⁻]_o = 10.8 mM, J_H = 17.5 pmol cm⁻² s⁻¹). The data at other pH_o values were fitted by the Michaelis-Menten equation. *n* is the number of data points fitted.

pH_o 8.0 to 7.4 quadrupling $K_m(\text{Na}^+)$ as predicted by the ion pair model. The 0.6 pH unit decrease from pH_o 8.6 to 7.4 caused $K_m(\text{Na}^+)$ to increase by a factor of somewhat less than 2.5. Thus, just as was the case for the pH_o dependence of $K_m(\text{HCO}_3^-)$, the pH_o dependence of $K_m(\text{Na}^+)$ was somewhat smaller than expected in the highest pH_o range examined.

DISCUSSION

Summary

An analysis of the effects of pH_o changes on the Na⁺-dependent Cl-HCO₃ exchanger is important both because pH_o disturbances are common, and because the transporter is a key player in the regulation of pH_i in both invertebrate and vertebrate cells. In approaching this study, we had five major goals. The first was to confirm the observation, previously made only on barnacle muscle fibers (Boron, McCormick, and Roos, 1979), that graded decreases in pH_o produce graded inhibitions of Na⁺-dependent Cl-HCO₃ exchange. The results, summarized in Fig. 2A, indicate that metabolic acid-base disturbances have a sizable effect on the transporter, with an apparent pK of ~7.7 and a Hill coefficient of nearly 3.

Our second goal was to examine the effects of respiratory acid-base disturbances on Na⁺-dependent Cl-HCO₃ exchange. To our knowledge, such an analysis had not been done. As summarized in Fig. 2B, we found that graded decreases of pH_o at a fixed [HCO₃⁻]_o produce graded inhibitions of transport. The maximal steepness of the relationship between J_H and pH_o, however, is less than half as great as with metabolic acid-base disturbances.

Third, we wished to examine how the exchanger responds to pH_o changes made at a fixed [NaCO₃⁻]_o. Therefore, we introduced two novel methods for varying pH_o: (i) we fixed [NaCO₃⁻]_o (and [CO₃⁻]_o) by making appropriate changes in both [CO₂]_o and [HCO₃⁻]_o; and (ii) we fixed [NaCO₃⁻]_o (and [HCO₃⁻]_o) by appropriately changing [CO₂]_o and [Na⁺]_o. We were surprised to find that the transporter is minimally affected by pH_o changes made by either of these two methods (see Fig. 2, C and D).

Our fourth goal was to assess how pH_o changes affect the apparent K_m and J_{\max} values obtained when varying [Na⁺]_o, [HCO₃⁻]_o, [CO₃⁻]_o, or [NaCO₃⁻]_o. As summarized in Tables IV–VI, none of the J_{\max} values is substantially affected by pH_o changes. However, both $K_m(\text{Na}^+)$ and $K_m(\text{HCO}_3^-)$ approximately halve for each pH_o increase of 0.3 in the pH_o range 7.1–8.3 (Tables IV and VI). On the other hand, both $K_m(\text{CO}_3^-)$ and $K_m(\text{NaCO}_3^-)$ are virtually insensitive to these pH_o changes (see Tables III and V).

Our final goal was to use the data summarized above in an attempt to determine whether it is HCO₃⁻, CO₃⁻ or NaCO₃⁻ that is the base transported by the Na⁺-dependent Cl-HCO₃ exchanger. The results of this analysis are summarized below.

Mechanisms by Which pH_o Changes Are Expected to Affect Na⁺-dependent Cl-HCO₃ Exchange

pH_o changes could affect the Na⁺-dependent Cl-HCO₃ exchange rate in at least two ways. First, they could alter the degree of protonation of titratable groups near the transporter's extracellular surface. In principle, such direct effects could cause a pH_o

decrease to inhibit, stimulate, or have no influence on transport. Second, pH_o changes could affect the transport rate by altering the concentration of the transported base (i.e., HCO₃⁻, CO₃⁼, or NaCO₃⁻). Neglecting direct pH_o effects, all four models of Na⁺-dependent Cl-HCO₃ exchange (see Introduction) predict that a pH_o decrease should inhibit transport only if the pH_o decrease caused a fall in the concentration of the transported base. Thus, the total effect of a pH_o shift on transport should have two components, the direct effect on the transporter's titratable groups, and the substrate effect. Varying pH_o in different ways might provide insight into the mechanism of transport.

Predicted Effects of pH_o Changes for Different Models of Na⁺-dependent Cl-HCO₃ Exchange

In three previous kinetic studies of the axon's Na⁺-dependent Cl-HCO₃ exchanger, the approach was to examine how J_H is affected by changes in [HCO₃⁻]_o and/or [Na⁺]_o in the absence or presence of DNDS. Because these earlier studies were all performed at the single pH_o of 8.0, changes in [HCO₃⁻]_o produced proportional changes in [CO₃⁼]_o. The results of these earlier studies were always consistent with the ion pair model, but did not rule out highly restricted versions of models involving the ordered or random binding of Na⁺ and HCO₃⁻ (or CO₃⁼) (Boron and Knakal, 1989).

HCO₃⁻. We will now consider if the data of series 1–series 4 can be reconciled with the hypothesis that HCO₃⁻ itself is the base transported by the Na⁺-dependent Cl-HCO₃ exchanger. We shall assume that HCO₃⁻ interacts with the transporter only as a substrate, and that neither CO₃⁼ nor NaCO₃⁻ interact with the transporter. The data from series 1 show that when pH_o and [HCO₃⁻]_o are reduced at a fixed [CO₂]_o, there is a steep fall in J_H . This could be due entirely to the decrease in substrate concentration (i.e., [HCO₃⁻]_o), or to a combination of decreased [HCO₃⁻]_o and a direct inhibitory effect of low pH_o.

The series 2 experiments show that reducing pH_o at a fixed [HCO₃⁻]_o causes a fall in J_H that is less steep than when pH_o and [HCO₃⁻]_o are reduced simultaneously (series 1). Thus, if HCO₃⁻ is the substrate, the shallow J_H vs. pH_o profile in the series 2 experiments (Fig. 2 B) represents the direct effect on the transporter of varying pH_o, the kinetic counterpart of which would be an effect on the affinity for HCO₃⁻. As indicated in Table IV, decreasing pH_o from 8.6 to 7.1 (at a fixed [Na⁺]_o of 425 mM) elicits only minor changes in $J_{\max}(\text{HCO}_3^-)$, but causes $K_m(\text{HCO}_3^-)$ to increase from 1 to 26.7 mM. Based on the best-fit parameters in Table IV, we predict that decreasing pH_o from 8.6 to 7.1 at a fixed [HCO₃⁻]_o of 12 mM should cause J_H to fall from 21.8 to 8.2 pmol cm⁻² s⁻¹, similar to the results summarized in Fig. 2 B and Table II. These same kinetic parameters also account for the series 1 data, predicting that decreasing pH_o from 8.6 to 7.1 by decreasing [HCO₃⁻]_o from 48 to 1.5 mM at a fixed [CO₂]_o of 0.5% should cause J_H to decrease from 23.1 to 1.4 pmol cm⁻² s⁻¹, similar to our results (Fig. 2 A and Table II).

In the series 3 experiments the reduction of pH_o from 8.6 to 7.1 was accomplished by increasing [HCO₃⁻]_o by ~32-fold but decreasing [CO₂]_o by ~1,000 fold. This combination of maneuvers had no effect on J_H . If HCO₃⁻ were the true substrate of the transporter, then decreasing pH_o from 8.6 to 7.1 must have had offsetting effects on $K_m(\text{HCO}_3^-)$ (i.e., a direct effect) and [HCO₃⁻]_o (i.e., a substrate effect). Indeed,

although this pH_o decrease caused $K_m(\text{HCO}_3^-)$ to increase from 1 to 26.7 mM (see Table IV), there was a corresponding increase in $[\text{HCO}_3^-]_o$, from 3 to 96 mM (see Table II). Based on the best-fit parameters in Table IV, we predict that decreasing pH_o from 8.6 to 7.1 while increasing $[\text{HCO}_3^-]_o$ from 3 to 96 mM should cause J_H to change from 17.7 to 20.7 $\text{pmol cm}^{-2} \text{ s}^{-1}$, similar to our data (Fig. 2 C and Table II). Thus, the series 3 data do not rule out the HCO_3^- model.

In the series 4 experiments, the reduction of pH_o from 8.6 to 7.1 was accomplished by increasing both $[\text{CO}_2]_o$ and $[\text{Na}^+]_o$ by ~ 32 -fold at fixed levels of $[\text{NaCO}_3^-]_o$ and $[\text{HCO}_3^-]_o$. These maneuvers had only minor effects on J_H . Because $[\text{HCO}_3^-]_o$ was fixed, HCO_3^- could be the true substrate of the transporter only if our method of decreasing pH_o from 8.6 to 7.1 did not alter $K_m(\text{HCO}_3^-)$. Although the kinetic parameters summarized in Table IV indicate that $K_m(\text{HCO}_3^-)$ approximately doubles for each 0.3 fall in pH_o , this analysis was based on data obtained at a fixed $[\text{Na}^+]_o$ of 425 mM. In our experiments, each 0.3 fall in pH_o was accompanied by a doubling of $[\text{Na}^+]_o$. Earlier work (Boron, 1985) at the single pH_o of 8.0 has established that $K_m(\text{HCO}_3^-)$ is approximately inversely proportional to $[\text{Na}^+]_o$. If this relationship between $K_m(\text{HCO}_3^-)$ and $[\text{Na}^+]_o$ holds at other pH_o values between 7.1 and 8.6, then the tendency of a pH_o decrease in series 4 to raise $K_m(\text{HCO}_3^-)$ would be offset exactly by the tendency of a $[\text{Na}^+]_o$ increase to lower $K_m(\text{HCO}_3^-)$. Thus, it is not unreasonable to hypothesize that the apparent $K_m(\text{HCO}_3^-)$ was stable in the series 4 experiments. If this were true, then the series 4 data, as were the data from series 1–series 3, would be consistent with the model that HCO_3^- itself is the transported base.

CO_3^{2-} . In testing the hypothesis that CO_3^{2-} is the transported base, we shall assume that neither HCO_3^- nor NaCO_3^- interact with the transporter. In the series 1 experiments, a pH_o decrease is accompanied by a very large reduction in $[\text{CO}_3^{2-}]_o$ ($\sim 1,000$ -fold when pH_o falls from 8.6 to 7.1), and a steep fall in J_H . Although, in principle, low pH_o could inhibit transporter directly, examination of Table V shows that the apparent K_m and J_{max} values for CO_3^{2-} at a fixed $[\text{Na}^+]_o$ of 425 mM are fairly insensitive to changes in pH_o between 7.1 and 8.6. Thus, if CO_3^{2-} were the substrate, we would expect all of the inhibition in series 1 to reflect a decrease in substrate concentration. Based on the kinetic parameters in Table V, we predict that decreasing pH_o from 8.6 to 7.1, accompanied by a decrease in $[\text{CO}_3^{2-}]_o$ from 1,911 to 1.9 μM , should cause J_H to fall from 23.1 to 1.4 $\text{pmol cm}^{-2} \text{ s}^{-1}$, similar to our data (Fig. 2 A and Table II).

In the series 2 experiments, decreasing pH_o is accompanied by a smaller reduction in $[\text{CO}_3^{2-}]_o$ (~ 32 -fold when pH_o falls from 8.6 to 7.1) and causes a decrease in J_H that is less steep than in series 1. Because the kinetic parameters for CO_3^{2-} are relatively pH_o insensitive, we expect this inhibition to reflect a decrease in $[\text{CO}_3^{2-}]_o$ itself. Based on the parameters in Table V, we predict that decreasing pH_o from 8.6 to 7.1, accompanied by a decrease in $[\text{CO}_3^{2-}]_o$ from 478 to 14.8 μM , should cause J_H to fall from 21.7 to 8.1 $\text{pmol cm}^{-2} \text{ s}^{-1}$, similar to our data (Fig. 2 B and Table II). Thus, the J_H data from series 1 and series 2 are consistent with the hypothesis that CO_3^{2-} is the substrate and that the difference between Figs. 2 A and 2 B reflects the smaller changes in $[\text{CO}_3^{2-}]_o$ in the latter case.

The series 3 experiments saw no change in either $[\text{CO}_3^{2-}]_o$ or J_H as pH_o was reduced from 8.6 to 7.1. If CO_3^{2-} is indeed the transporter's substrate, these data indicate that

the transporter is virtually insensitive to pH_o changes between 7.1 and 8.6, consistent with the kinetic parameters summarized in Table V, which indicate that $K_m(\text{CO}_3^-)$ and $J_{\max}(\text{CO}_3^-)$ are relatively insensitive to pH_o changes in this pH_o range.

In the series 4 experiments, reducing pH_o from 8.6 to 7.1 had no effect on J_H even though $[\text{CO}_3^-]_o$ was reduced by a factor of > 32 . Although this seems inconsistent with the CO_3^- model, $[\text{CO}_3^-]_o$ decrease was accompanied by a corresponding increase in $[\text{Na}^+]_o$ (Table I). As noted above, earlier work at pH_o 8.0 showed that J_H is unaffected by reciprocal alterations in $[\text{Na}^+]_o$ and $[\text{HCO}_3^-]_o$ (or $[\text{CO}_3^-]_o$) that leave the product $[\text{Na}^+]_o \times [\text{HCO}_3^-]_o$ (or $[\text{Na}^+]_o \times [\text{CO}_3^-]_o$) unchanged. If a similar relationship between $[\text{Na}^+]_o$ and $K_m(\text{HCO}_3^-)$ or $K_m(\text{CO}_3^-)$ holds for all pH_o values between 7.1 and 8.6, then these series 4 data would be consistent with the model that CO_3^- is the extracellular substrate. Thus, the series 1–series 4 data do not rule out the model that CO_3^- is the transporter's substrate.

NaCO₃⁻. In considering that NaCO_3^- is the transporter's substrate, we shall assume that neither HCO_3^- , CO_3^- , nor Na^+ interact with the transporter. The analysis of the series 1 and series 2 experiments in terms of the NaCO_3^- ion pair model is virtually the same as for the CO_3^- model discussed above. In brief, the data summarized in Table III show that the apparent K_m and J_{\max} values for NaCO_3^- are fairly insensitive to changes in pH_o between 7.1 and 8.6. The difference between the steepness of the J_H vs. pH_o relationships in Figs. 2A and 2B could be accounted for by the smaller changes in $[\text{NaCO}_3^-]_o$ in the latter case. Thus, these data are consistent with the ion pair model.

The series 3 and series 4 data are also consistent with the NaCO_3^- ion pair model. In both cases, the reduction in pH_o from 8.6 to 7.1 was achieved with no change in $[\text{NaCO}_3^-]_o$ and was accompanied by no change in J_H . In summary, if NaCO_3^- is indeed the substrate, the data from series 1–series 4 would require that the transporter's kinetic parameters be virtually unaffected by changes in pH_o between 7.1 and 8.6, as supported by the data of Table III.

Conclusions

Ad hoc assumptions required by the HCO₃⁻ and CO₃⁼ models. Although the NaCO_3^- ion pair model remains the most straightforward explanation for our data, we cannot rule out models with HCO_3^- or CO_3^- as the transported base. However, if either HCO_3^- or CO_3^- is the substrate, then our kinetic data (Tables III–VI) require that additional restrictions be placed upon allowable kinetic parameters. Moreover, at least one series of ad hoc assumptions must be imposed for either the HCO_3^- or the CO_3^- model to be viable.

In the case of the HCO_3^- model, two ad hoc assumptions are required. First, the series 3 data can be explained only if the ~ 32 -fold increase in $[\text{HCO}_3^-]_o$ that accompanied the decrease in pH_o from 8.6 to 7.1 is matched by comparable changes in $K_m(\text{HCO}_3^-)$. Also, the series 4 data can be explained only if $K_m(\text{HCO}_3^-)$ is inversely proportional to $[\text{Na}^+]_o$ over the pH_o range 7.1–8.6. A question that arises is whether fulfilling these two ad hoc assumptions would be overly serendipitous. Both assumptions are predictions of the NaCO_3^- ion pair model.

In the case of the CO_3^- model, one ad hoc assumption is required to explain the

series 4 data: $K_m(\text{CO}_3^{=})$ would have to be inversely proportional to $[\text{Na}^+]_o$ at all pH_o values between 7.1 and 8.6. This is a prediction of the NaCO_3^- ion pair model.

Model-independent conclusions. Although the preceding discussion is model dependent, our data lead to two important model-independent conclusions. First, because J_{max} values are remarkably insensitive to pH_o changes, inhibition of Na^+ -dependent Cl-HCO_3^- exchange by low pH_o can be overcome by increasing the level of a substrate (i.e., Na^+ , HCO_3^- , $\text{CO}_3^{=}$, or NaCO_3^-). Second, the exchanger behaves as if J_H were governed uniquely by the product $[\text{Na}^+]_o \times [\text{CO}_3^{=}]_o$ (as predicted by the ion pair model). That is, the transporter behaves as if $[\text{HCO}_3^-]_o$ and pH_o were inconsequential, and as if $[\text{Na}^+]_o$ and $[\text{CO}_3^{=}]_o$ were important only insofar as they determine the product $[\text{Na}^+]_o \times [\text{CO}_3^{=}]_o$.

Unanswered kinetic questions. As pointed out previously (Boron and Knakal, 1989), if kinetic data are consistent with the ion pair model, it will always be possible to fit the data with models calling for the random or ordered binding of Na^+ and $\text{CO}_3^{=}$ or HCO_3^- . The reason is that the binding of one substrate (e.g., Na^+) could sufficiently raise the transporter's affinity for the second substrate (e.g., $\text{CO}_3^{=}$), such that the binding of one would be tantamount to the binding of both substrates. Thus, it will be impossible to rule in the ion pair model to the exclusion of the other models. One approach for evaluating models of Na^+ -dependent Cl-HCO_3^- exchange would be to continue to gather data in the hope of making an observation inconsistent with the ion pair model. At least three major categories of experiments are suggested by the present work. The first involves testing the predictions made by the ion pair model about the dependence of $K_m(\text{HCO}_3^-)$ on $[\text{Na}^+]_o$ and the dependence of $K_m(\text{Na}^+)$ on $[\text{HCO}_3^-]_o$ at pH_o values other than 8.0. These data on $K_m(\text{HCO}_3^-)$ and $K_m(\text{Na}^+)$ would also permit a thorough evaluation of the models involving the binding of Na^+ and HCO_3^- . Second, one could test the predictions of the ion pair model concerning the dependence of $K_m(\text{Na}^+)$ on pH_o at a fixed $[\text{CO}_3^{=}]_o$, as well as the dependence of $K_m(\text{Na}^+)$ on $[\text{CO}_3^{=}]_o$ over a range of pH_o values. Such data, not obtained in this study, would permit a full analysis of the model involving the binding of Na^+ and $\text{CO}_3^{=}$. Finally, one could vary pH_o by means other than those used in series 1–series 4.

This work was supported by NIH grant NS-18400.

Original version received 22 April 1991 and accepted version received 9 January 1992.

REFERENCES

- Boron, W. F. 1985. Intracellular pH-regulating mechanism of the squid axon. Relation between the external Na^+ and HCO_3^- dependences. *Journal of General Physiology*. 85:325–345.
- Boron, W. F., and P. De Weer. 1976. Active proton transport stimulated by $\text{CO}_2/\text{HCO}_3^-$ blocked by cyanide. *Nature*. 259:240–241.
- Boron, W. F., and R. C. Knakal. 1986. Dependence of the squid-axon intracellular pH regulating mechanism on extracellular pH. *Biophysical Journal*. 49:550a. (Abstr.)
- Boron, W. F., and R. C. Knakal. 1989. Intracellular pH-regulating mechanism of the squid axon: interaction between DNDS and extracellular Na^+ and HCO_3^- . *Journal of General Physiology*. 93:123–150.

- Boron, W. F., W. C. McCormick, and A. Roos. 1979. pH regulation in barnacle muscle fibers: dependence on intracellular and extracellular pH. *American Journal of Physiology*. 237:C185–C193.
- Boron, W. F., W. C. McCormick, and A. Roos. 1981. pH regulation in barnacle muscle fibers: dependence on extracellular sodium and bicarbonate. *American Journal of Physiology*. 240:C80–C89.
- Boron, W. F., and J. M. Russell. 1983. Stoichiometry and ion dependencies of the intracellular-pH-regulating mechanism in squid giant axons. *Journal of General Physiology*. 81:373–399.
- Boyersky, G., M. B. Ganz, B. Sterzel, and W. F. Boron. 1988. pH regulation in single glomerular mesangial cells. II. Na-dependent and -independent Cl-HCO₃ exchangers. *American Journal of Physiology*. 255:C857–C869.
- Brinley, F. J., Jr., and L. J. Mullins. 1967. Sodium extrusion by internally dialyzed squid axons. *Journal of General Physiology*. 50:2303–2311.
- Cassel, D., O. Scharf, M. Rotman, E. J. Cragoe, Jr., and M. Katz. 1988. Characterization of Na⁺-linked and Na⁺-independent Cl⁻/HCO₃⁻ exchange systems in Chinese hamster lung fibroblasts. *Journal of Biological Chemistry*. 263:6122–6127.
- Hinke, J. A. M. 1967. Cation-selective microelectrodes for intracellular use. In *Glass Electrodes for Hydrogen and Other Cations: Principle and Practice*. G. Eisenman, editor. Marcel Dekker, Inc., New York. 464–477.
- L'Allemain, G., S. Paris, and J. Pouyssegur. 1985. Role of a Na⁺-dependent Cl⁻/HCO₃⁻ exchange in regulation of intracellular pH in fibroblasts. *Journal of Biological Chemistry*. 260:4877–4883.
- Moody, W. J., Jr. 1981. The ionic mechanism of intracellular pH regulation in crayfish neurones. *Journal of Physiology*. 316:293–308.
- Rothenberg, P., L. Glaser, P. Schlesinger, and D. Cassel. 1983. Activation of Na⁺/H⁺ exchange by epidermal growth factor elevates intracellular pH in A431 cells. *Journal of Biological Chemistry*. 258:12644–12653.
- Russell, J. M., and W. F. Boron. 1976. Role of chloride transport in regulation of intracellular pH. *Nature*. 264:73–74.
- Thomas, R. C. 1976. Ionic mechanism of the H⁺ pump in a snail neuron. *Nature*. 262:54–55.
- Thomas, R. C. 1977. The role of bicarbonate, chloride and sodium ions in the regulation of intracellular pH in snail neurones. *Journal of Physiology*. 273:317–338.
- Tonnessen, T. I., J. Ludt, K. Sandvig, and S. Olsnes. 1987. Bicarbonate/chloride antiport in vero cells: I. Evidence for both sodium-linked and sodium-independent exchange. *Journal of Cell Physiology*. 132:183–191.